Laboratory Research
J Korean Neurosurg Soc 66 (4) : 382-392, 2023
https://doi.org/10.3340/jkns.2022.0180
pISSN 2005-3711 eISSN 1598-7876

Numerical Model for Cerebrovascular Hemodynamics with Indocyanine Green Fluorescence Videoangiography

Hwayeong Cheon,[1] Young-Je Son,[2] Sung Bae Park,[2] Pyoung-Seop Shim,[3] Joo-Hiuk Son,[4] Hee-Jin Yang[2]

Biomedical Engineering Research Center,[1] Asan Institute for Life Sciences, Asan Medical Center, Seoul, Korea
Department of Neurosurgery,[2] Seoul National University Boramae Hospital, Seoul, Korea
System Configuration Team,[3] Korea Institute of Atmospheric Prediction Systems, Seoul, Korea
Department of Physics,[4] University of Seoul, Seoul, Korea

Objective : The use of indocyanine green videoangiography (ICG-VA) to assess blood flow in the brain during cerebrovascular surgery has been increasing. Clinical studies on ICG-VA have predominantly focused on qualitative analysis. However, quantitative analysis numerical modelling for time profiling enables a more accurate evaluation of blood flow kinetics. In this study, we established a multiple exponential modified Gaussian (multi-EMG) model for quantitative ICG-VA to understand accurately the status of cerebral hemodynamics.

Methods : We obtained clinical data of cerebral blood flow acquired the quantitative analysis ICG-VA during cerebrovascular surgery. Varied asymmetric peak functions were compared to find the most matching function form with clinical data by using a nonlinear regression algorithm. To verify the result of the nonlinear regression, the mode function was applied to various types of data.

Results : The proposed multi-EMG model is well fitted to the clinical data. Because the primary parameters—growth and decay rates, and peak center and heights—of the model are characteristics of model function, they provide accurate reference values for assessing cerebral hemodynamics in various conditions. In addition, the primary parameters can be estimated on the curves with partially missed data. The accuracy of the model estimation was verified by a repeated curve fitting method using manipulation of missing data.

Conclusion : The multi-EMG model can possibly serve as a universal model for cerebral hemodynamics in a comparison with other asymmetric peak functions. According to the results, the model can be helpful for clinical research assessment of cerebrovascular hemodynamics in a clinical setting.

Key Words : Cerebrovascular circulation · Vascular surgical procedures · Indocyanine green · Fluorescence angiography · Hemodynamic monitoring · Computer-assisted numerical analysis.

INTRODUCTION

Indocyanine green videoangiography (ICG-VA) is a renowned tool for providing relevant information on vascular blood flow of patients during cerebrovascular surgery[5,10,13,18,29,31]. Several medical research groups have employed ICG-VA in neu-

• Received : July 27, 2022 • Revised : September 19, 2022 • Accepted : September 22, 2022
• Address for correspondence : **Hee-Jin Yang**
Department of Neurosurgery, Seoul National University Boramae Hospital, 20 Boramae-ro 5-gil, Dongjak-gu, Seoul 07061, Korea
Tel : +82-2-870-2303, Fax : +82-870-3863, E-mail : nsyangdr@gmail.com, ORCID : https://orcid.org/0000-0002-6413-1363

rosurgery studies. Most of them have used ICG-VA to assess vascular blood flow with qualitative analysis based on angiography findings. Only a few quantitative analyses on ICG-VA involved measurement of the fluorescence intensity in the process of time[1,4,19,27]. Tempolabile quantitative analysis enables more accurate assessments of hemodynamics and can lead to a model for blood flow in body[17,34]. Some studies have strived to provide several model functions for blood flow in the brain[3,9,22,24,35]. However, determining blood flow in a clinical setting is difficult because the signal for the vascular blood flow time profile is highly variable depending on the conditions of patients, as described in other imaging modalities[36]. Thus, it is important to establish a vascular blood flow model that can be applied to various time profile signals for data to elucidate the kinetics of blood circulation in the brain and obtain principle parameters that enable evaluation of biological phenomena. These parameters include the number, time (or location of the center), height, and growth and decay rates of the peaks[17]. These parameters provide objective information to diagnose the vascular blood flow of patients and identify the distinctions among the hemodynamic mechanisms[15,20,21,28].

In this study, we demonstrated that cerebrovascular hemodynamics can be presented as a mathematical model that is an exponential modified Gaussian (EMG) function. The numerical model was shown to be well fitted to ICG-VA tempolabile quantitative data. The model was constructed using a fitting algorithm with nonlinear regression. We predicted the primary parameters of curves (center of peaks, height of peaks, growth rate, and decay rate from the data set) of data comprised of points missed partly by the measurement limitation.

MATERIALS AND METHODS

The study was approved by IRB of Seoul National University Boramae Hospital (30-2020-097). We obtained the curve data from ICG-VA during cerebrovascular surgery in conformity with our previous research[33]. We employed commercially available products for the ICG dye (Daiichi Sankyo, Tokyo, Japan) and surgical microscope (OPMI Pentero; Carl Zeiss Co., Oberkochen, Germany). The angiogram video was converted to static images using the video player and capture freeware (GomPlayer v. 2.1.36; Gretech Corp., Seoul, Korea). Tempolabile quantitative analysis data were extracted from the static image stacks by the multi-measure plug-in of ImageJ (v. 1.42q; http://rsb.info.nih.gov/ij/; National Institutes of Health, Bethesda, MD, USA).

The vascular blood flow circulatory system included the heart, lung, brain, and extra body[2]. ICG was injected as an intravenous bolus into the central venous line and was observed using an ICG-VA technique at the cerebral arteries. The measured signals were composed of absorption and elimination phases, and the time and width of the peaks in the time domain projected the kinetic information on the blood flow. Intravenous bolus injection formed an ideal pulse shape of the cerebrovascular hemodynamic curve between the absorption

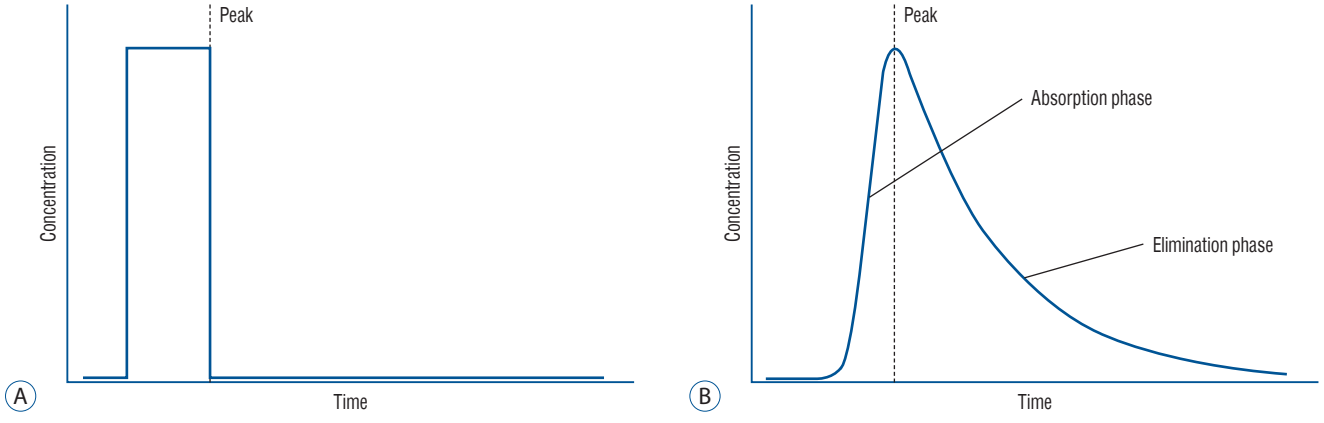

Fig. 1. Shapes of the intravenous bolus signal. Intravenous bolus injection may cause a pulse shape in the signal (A). However, the real measured cerebral hemodynamic curve may be changed to the asymmetry Gaussian function (B) because a rapid injection would increase the indocyanine green (ICG) concentration in a short period. Nevertheless, the ICG diffusion at the plasma level would be relatively slow. In other words, duration of the elimination phase is longer than that of the absorption phase in the peak function form.

and elimination phases (Fig. 1A). However, the measured curve had the shape to an asymmetry peak function, as shown in Fig. 1B, because of the injection distribution and dispersion effect. The quantity of the injected ICG could have a Gaussian distribution in practice on account of the random noise variance. Thus, the ICG concentration in the blood could increase under the cumulative distribution function (CDF) in the absorption phase.

After the bolus, the concentration was exponentially decayed by the dispersion effect[14]. Therefore, we assumed that the measured cerebrovascular hemodynamic curve ($CH_{measure}(t)$) was represented as follow.

$$CH_{measure}(t) = CDF(t) \times \exp(-t) \quad (1)$$

We chose the EMG model, which is one of the asymmetry peaks, as a candidate to fit on the curve. It has a similar mathematical express as Equation (1)[11]. The error function (erf) in the EMG could be transposed into CDF, Ø(t) with the following relationship.

$$\phi(t) = \frac{1}{2} + \frac{1}{2}\,\mathrm{erf}\left(\frac{t}{\sqrt{2}}\right) = \frac{1}{2} + \frac{1}{\sqrt{\pi}}\int_0^t e^{-x^2}\,dx \quad (2)$$

EMG was compared and evaluated to identify a suitable model function for the measurement data. The data were calculated by the Levenberg-Marquardt algorithm (nonlinear least-squares algorithm) using scientific graphing and data analysis software, Origin9 Pro (v. 9.0.0.; OriginLab Co., Northampton, MA, USA).

EMG model for the cerebrovascular hemodynamic curve

EMG has typically been used for both chromatographic distribution and peak analyses in a wide range of fields[8,12,23]. EMG is expressed by the convolution of one CDF Ø(t) and one exponential function (Equation [3]) :

$$EMG(t) = y_o + A\phi(z)\cdot\exp\left(\frac{1}{2}\left(\frac{w}{t_0}\right)^2 - \frac{(t-t_0)}{t_0}\right)$$
$$z(t) = \frac{(t-t_0)}{w} - \frac{w}{t_0} \quad (3)$$

where A is the peak amplitude, t_0 is the exponential relax-

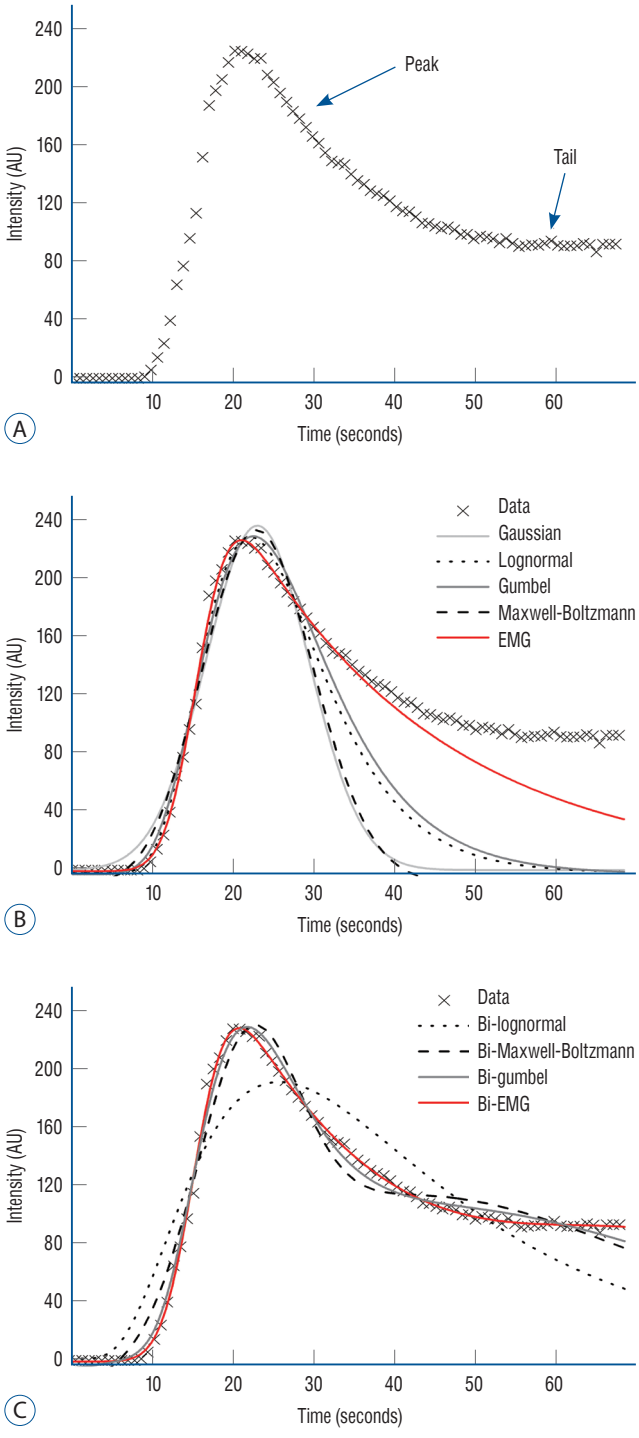

Fig. 2. Fitting results on the peak and whole areas of the indocyanine green videoangiography (ICG-VA) data curve. A : Standard shape of the quantitative ICG-VA clinical data. The number of peaks changed; however, the curve was mainly composed of peaks and a long tail. B : Comparison of the fitting curves with peak functions at the peak area. Exponential modified Gaussian (EMG; black line) fitted better than other peak functions (extra lines) on the shape of the peak. C : To include the tail part, the linear bi-summation of the peak functions was needed. Bi-EMG presented the best fitting curve on the whole data area.

 https://doi.org/10.3340/jkns.2022.0180

ation rate for decay, *w* is the variable related to the peak width and growth rate, and t_C is the variable related to the center of peaks.

The CDF with the sigmoid (S-shaped) form increases from 0 to 1. The parameter w is the growth steepness; thus, w means the growth rate degree. EMG is the convolution function. Meanwhile, CDF does not influence the elimination phase because the CDF value is only one in the elimination phase. In other words, CDF is dominant in the absorption phase, which is the growth part of the peak of the EMG curve. The exponential function is only related to the elimination phase, which is the decay part of the curve.

The decay rate degree enables defining the decay constant of the exponential function, $\frac{1}{t_0}$, as shown in Fig. 2. Consequently, we employ four primary parameters to determine the peaks in the EMG, which, in turn, determines the shape of the peaks, steepness of the CDF or growth rate of the peaks, w, decay constant of the peaks, $\frac{1}{t_0}$, and size and location of the peaks (height and center of peaks).

RESULTS

To evaluate the validity of the EMG model, the R-squared value was compared with other peak functions and a bi-summation of the peak functions using the fitting algorithm. The applied data had a general form of a single peak, which was one of the quantitative ICG-VA clinical data. The number of frames in the X-axis of all measured data was transformed into the time domain to verify the data time profile.

We chose five peak functions : Gaussian function (G(t)), which is not actually an asymmetric peak function; nevertheless, it is the simplest function among the peak functions; log-normal function (L(t)) Gumbel distribution function (GB(t)); Maxwell-Boltzmann function (MB(t)); and EMG function (EMG(t)). Each function can be expressed as :

$$G(t) = y_0 + A\exp\left(-\left(\frac{t-t_c}{w}\right)^2\right) \quad (4)$$

$$L(t) = y_0 + \left(\frac{A}{wt}\right)\exp\left(-\frac{\ln(t/t_c)^2}{2w^2}\right) \quad (5)$$

$$GB(t) = y_0 + A\exp\left(-\exp\left(\frac{t-t_c}{w}\right)-\left(\frac{t-t_c}{w}\right)+1\right) \quad (6)$$

$$MB(t) = y_0 + Ax^2\exp\left(-\frac{(t-t_c)^2}{w}\right) \quad (7)$$

where y_0s are the offsets, A the amplitude of the peaks, w the width of the peaks, and t_C denotes the center of peaks.

Comparison with other fitting functions

Fig. 2A shows the cerebrovascular hemodynamic data in the time domain. It is comprised of clinical data with a common form of a single peak in the quantitative ICG-VA with the time profile. Specifically, it consists of a peak and a long-range tail. We fitted the clinical data from the peak area (up to the half-maximum of the peak in the elimination phase) to the whole data area because a peak function could not cover the whole data. It indicated that the signals required two or more functions to fit the whole data. Furthermore, the tail part should be applied with the same function in the peak area because the circulation system could not be changed while the signal was measured. Therefore, a high possibility existed that the whole data curve of the single peak would be fitted by linear bi-summations of the peak functions. Fig. 2B presents the fitting results of the five peak functions. All linear bi-summation functions fitted as shown in Fig. 2C. To compare the results, we calculated the R-squared values as shown in Table 1. We excluded the result of the bi-Gaussian function because it

Table 1. Comparison of the R-squared values according to the fitting region (region of the peak and whole area)

Region of the peak	R-squared	Whole data	R-squared
Gaussian function	0.9714	-	
Lognormal function	0.9940	Bi-lognormal function	0.8325
Gumbel function	0.9887	Bi-MB function	0.9648
Maxwell-Boltzmann (MB) function	0.9350	Bi-gumbel function	0.9908
EMG function	0.9978	Bi-EMG function	0.9973

EMG : exponential modified Gaussian

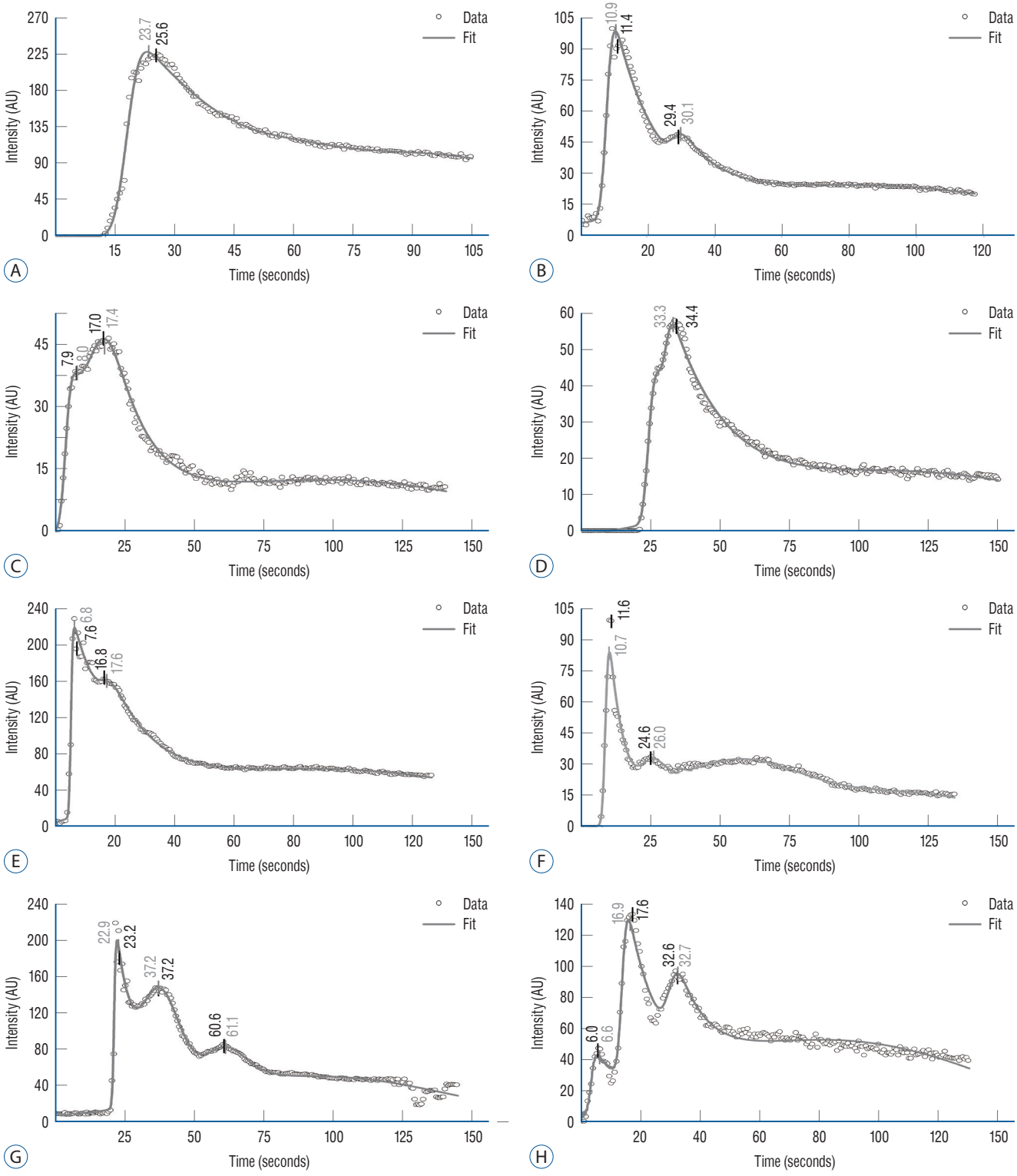

Fig. 3. Fitting curves (grey line) for the measurement data (open circle) of various forms using the multi- exponential modified Gaussian (EMG) model. A-H : Various shapes of the cerebral hemodynamic curves for vascular blood flow are observed. The curves are fitted by the multi-EMG function. The number of EMG functions required for effective fitting is one more than the number of peaks. The measured data are applied with a low-degree Savitzky-Golay filter to remove the fluctuation of data and ease the derivation. Each center of peaks defined by the point of the first derivative values is equal to zero at the local peaks. The center of peaks of the fitting curves (grey numbers) are substantially accorded with the ones (black numbers) of their measured data.

 https://doi.org/10.3340/jkns.2022.0180

was too deviated to fit on the curve.

The clinical data provided the best fit to the EMG function on both the peak and whole data area (Table 1). This result demonstrated that the multi-EMG function was required for fitting on multiple peak curves. The same number of EMG functions was needed; the peak and tail parts required only one.

Multi-EMG modelling for ICG curve

The bi-EMG function was well suited to expressing the single peak data with the time profile. We verified whether the multi-EMG function would fit on various forms of the signals. We collected several quantitative ICG-VA signals, which had a couple of peaks and a tail intact and varied depending on the status of the blood flow. Furthermore, we evaluated the multi-EMG model as the universal fitting function for the cerebrovascular hemodynamic curve (Fig. 3). The signals were fitted to ter- or quad-EMG, specifically three or four respective linear summations of EMG. The R-squared values revealed that the multi-EMG functions fitted well with the various forms of data (average value, 0.9832).

In addition, we identified the center of peaks at the peak area of the fitting curve and measured data using the peak-finding algorithm with the first derivative method. The first derivative values of the given function were equal to zero at the local peak point. The low degree Savitzky-Golay filter, one of the smoothing filters, was applied to the measured data while finding the center of peaks. The location of the center of peaks at the time axis in the fitting curve (grey numbers) was similar to that of the measured data (black numbers). Therefore, we could distinguish the center of peaks in the clinical data from one in the multi-EMG function.

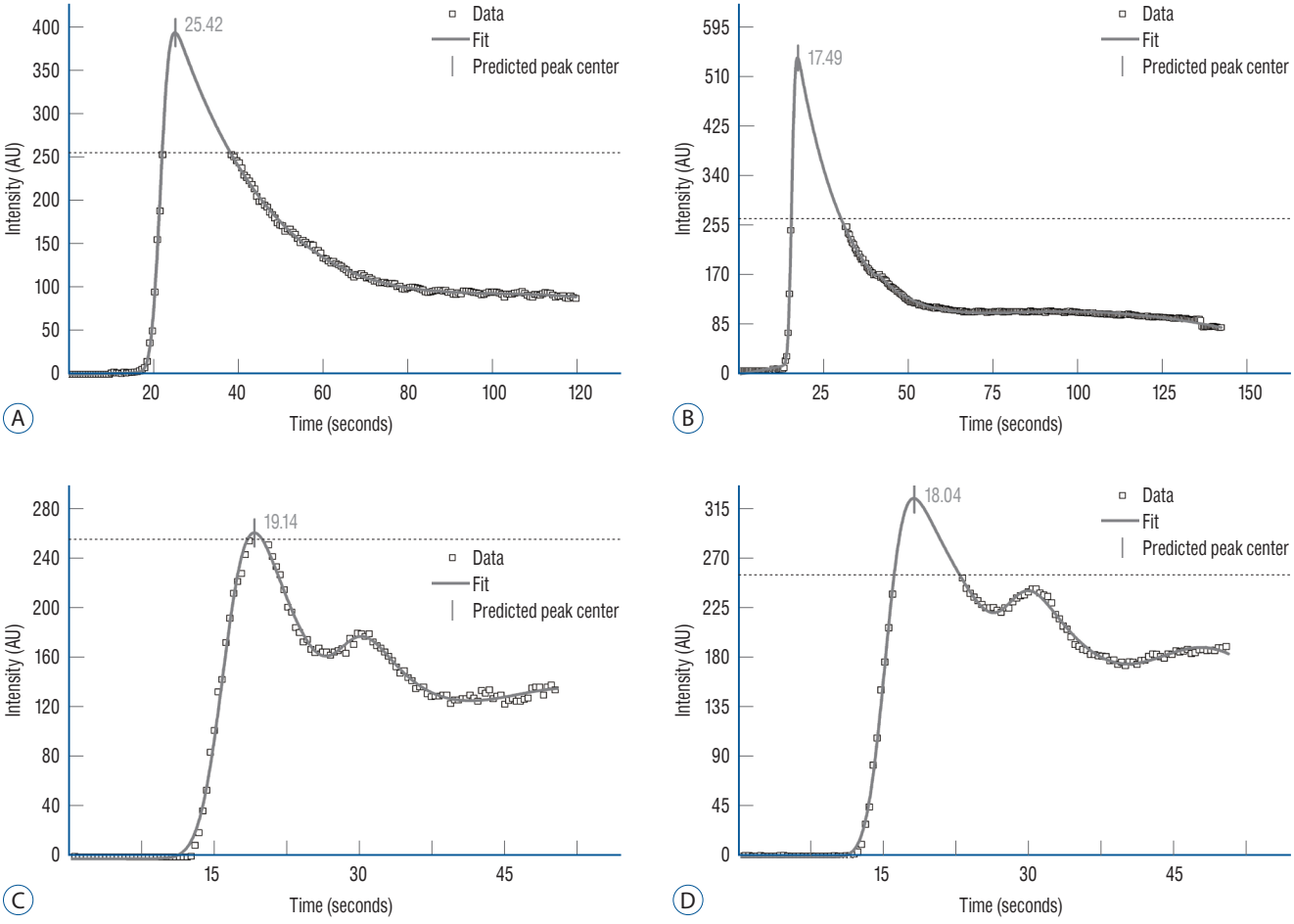

Fig. 4. Prediction of center of peaks on data (open circles) with missing parts. A-D : Some data points can be missed from saturation owing to the measuring equipment limitation. The fitting model (grey line; multi-EMG model) provides the estimated values of the parameter, center of peaks (grey numbers), and data. EMG : exponential modified Gaussian.

The partial data were sometimes missed, which may have been occurred when the intensity of the signal exceeded the measurement system limit. The fitting model restored the parameters of the particular missing data through the data trend. Fig. 4 shows that the multi-EMG model recovered the missing data and predicted center of peaks that could not be identified on the original measured data. To identify the predicted center of peaks, we used the same method with the fitting functions of non-saturated data.

DISCUSSION

In the evaluation, the numerical model of the quantitative ICG-VA provided accurate information on cerebrovascular hemodynamics and enabled a comparison of the blood flow in various conditions by using the primary parameters. The multi-EMG function was the best numerical function for reflecting cerebrovascular hemodynamics, which was proved using a nonlinear regression fitting algorithm. The number of EMG functions in multi-EMG was determined by the number of peaks in the clinical data. This is because the peak and tail were required for each component of the EMG function. For each peak, one component of the EMG function was dominant.

Fig. 5A shows the two component EMG functions composed of a single peak fitting function. The peak area of the fitting curve is predominantly influenced by the growth part of the first EMG. In terms of the logarithmic scale of the curve (Fig. 5B), the decay part of the peak area aligns with the exponential line in the first EMG. As shown in these figures, the first EMG component is dominant in the peak area; the second strongly influences the tail part. Therefore, we considered a relevant single EMG to analyse the properties of each peak.

An objective of curve fitting with nonlinear regression is to set a numerical model describing a complex biological system using equations and numerical parameters. The numerical models enable interpretation of the measured data as understandable systems and estimation of the parameters or trends of curves. Moreover, if data are missing from the "valid part"—which may be caused by the determination constraint in the measurement system—the model not only predicts the parameter, but it also restores the missing data to some extent[16].

Thus, to evaluate the model's effectiveness in data restoration, we maintained the top of the main peak from 60% to 100% in the real measured data based on the peak height (Fig. 6A and C). In the simulation, the intensity of the measurement signals exceeded the observable maximum of the ICG-VA system, as shown in Fig. 6. We reconstructed the missing parts at each truncated main peak (Fig. 6B and D) by applying the multi-EMG model. In addition, we estimated the primary parameters (center of peaks, peak height, steepness of growth (w), and the decay constant ($\frac{1}{t_0}$)) in the first EMG of the multi-EMG function that expressed the main peak.

Fig. 6E presents the relative difference based on the parame-

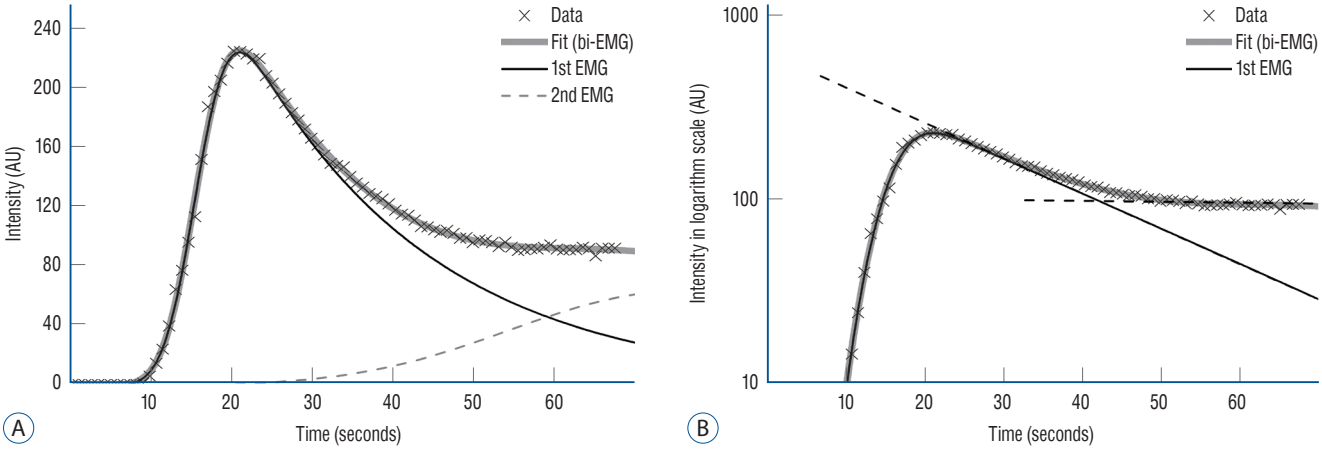

Fig. 5. Dominance of a single EMG function on each peak area. A : Fitting curve (grey line) of the multi-EMG for the clinical data and each component EMG (black line and grey dashed line). B : The same curve in the logarithmic scale. The black dashed lines show the exponential line in the logarithmic scale. The growth and decay parts of the peak predominantly match the first EMG. Therefore, the single EMG, which is the first EMG in this case, is dominant at the peak area. The peak properties can be obtained by analysing the first EMG. EMG : exponential modified Gaussian.

 https://doi.org/10.3340/jkns.2022.0180

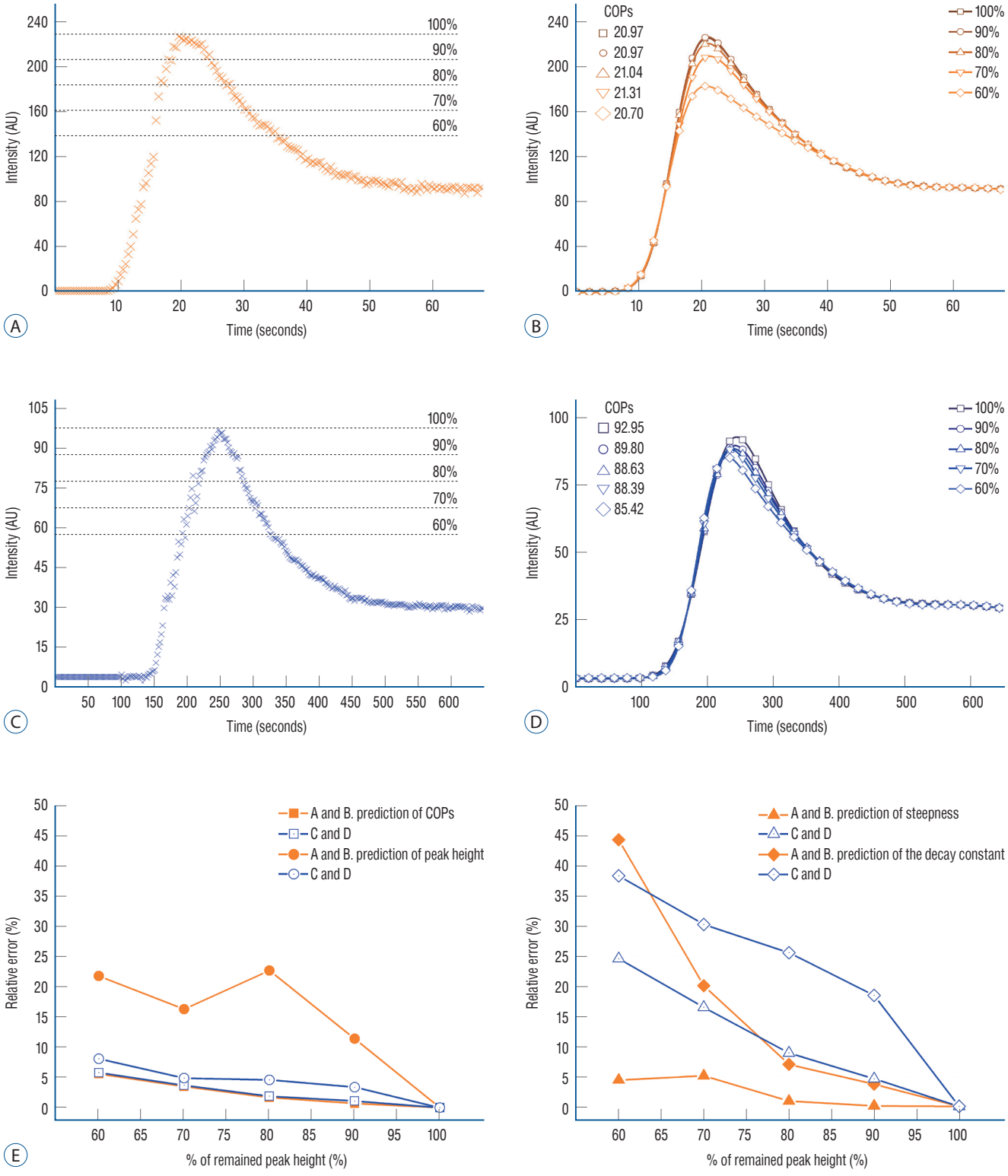

Fig. 6. Evaluation of multi-EMG model reconstruction. A and B : To check the model validity, the top of the main peak in the measured data was removed from 0% to 40% based on the peak height. C and D : Reconstructed data curve by the multi-EMG model. E : Comparison with the relative error of the estimated four primary parameters : center of peaks, peak height, steepness of growth (w), and decay constant ($\frac{1}{t_0}$). The smaller is the area of missing data, the more accurate is the prediction of the reconstructed parameters in all parameters. COP : center of peak, EMG : exponential modified Gaussian.

ters of the original fitting function. The accuracy of the reconstruction of all parameters is usually lower when the larger missing parts exist; however, the accuracy has a <30% margin of error if the peak remains greater than 70%. The decay constant has a relatively lower accuracy than the growth steepness because the larger missing parts influence the second EMG located in the tail part. However, the decay constant values are reliable if there are small missing areas, making it a possible evaluation value for the properties of the elimination phase.

There are other methods for assessment of hemodynamics using ICG-VA. Flow 800 (Carl Zess, Oberkochen, Germany) is a well-known software and there are several reports on its use in cerebrovascular surgery[6,32]. It is convenient for surgeons, without requiring any calculation by users. However, because the software can only calculate the delay and the slope (average intensity, AI/second) at a specific point of the intensity graph within the range arbitrarily determined by the clinician or researcher, there is a limit to obtain accurate quantitative values[7]. Our method provides the coefficient of fitting function based on nonlinear regression analysis, and it offers more objective evaluation indicators. Moreover, the commercial software is an integrated part of the operative microscope, compatible models were launched on 2011 and of considerable price (approximately 30 million Korean Won). Besides, it is impossible for analysis of data acquired in older model of microscope.

Considering the pros and cons of the commercial software and our methods, it might be said : commercial software is useful for intraoperative assessment for hemodynamics on site, whereas our methods for analysis for data in batch mode, especially for archived data to elucidate hemodynamic features of series of cases in more objective way with better accuracy.

The above results showed that the multi-EMG model reconstructed missing peak parameters with reliable prediction in the smaller missing area. The predicted values of the center of peaks in Fig. 6 are acceptable for the quantitative analysis of ICG-VA.

CONCLUSION

Establishing a numerical model for analysing a biological system has several advantages[25,26]. First, a mathematical model enables visualisation and intuitive comprehension of biological phenomena[30]. Biological phenomena usually occur as a result of combined reactions to a complex system. The numerical model developed in this study simplifies a given phenomenon into several equations and parameters. Through an analysis of these equations and parameters, the complex system can then be understood. Second, the trend and response of a phenomenon can be predicted as presented by the restoration of data in our series. Furthermore, the tempolabile quantitative analysis presents a time profile of vascular blood flow and enables a more accurate evaluation.

Based on the results of this study, the multi-EMG model can be used as a mathematical model for cerebrovascular hemodynamics to understand vascular blood flow, which is quantitatively measured by ICG-VA during cerebrovascular surgery. The proposed multi-EMG model fitted well in various conditions of vascular blood flow by nonlinear regression and reflected the parameters (such as center of peaks) of clinical data. Furthermore, we proved that the multi-EMG model reconstructed a portion of missing data and predicted the parameters of these missing parts. Our numerical model can thus enhance the insight of cerebrovascular hemodynamics in various clinical conditions.

AUTHORS' DECLARATION

Conflicts of interest

Hee-Jin Yang has been editorial board of JKNS since May 2020. He was not involved in the review process of this original article. No potential conflict of interest relevant to this article was reported.

Informed consent

This type of study does not require informed consent.

Author contributions

Conceptualization : HJY, HC; Data curation : HJY, HC, PSS; Formal analysis : HJY, HC, PSS; Funding acquisition : HJY, JHS; Methodology : HJY, HC, PSS; Project administration : HJY; Visualization : HJY, HC; Writing - original draft : HC, YJS, SBP, PSS, JHS, HJY; Writing - review & editing : HC, YJS, SBP, PSS, JHS, HJY

 https://doi.org/10.3340/jkns.2022.0180

Data sharing

The datasets used and/or analysed during the current study available from the corresponding author on reasonable request.

Preprint

None

ORCID

Hwayeong Cheon	https://orcid.org/0000-0001-6181-7768
Young-Je Son	https://orcid.org/0000-0002-8702-9804
Sung Bae Park	https://orcid.org/0000-0002-4652-3056
Pyoung-Seop Shim	https://orcid.org/0000-0003-4895-6338
Joo-Hiuk Son	https://orcid.org/0000-0002-5079-2531
Hee-Jin Yang	https://orcid.org/0000-0002-6413-1363

- Acknowledgements

This work was partly supported by the National Research Foundation of Korea (NRF) grant funded by the Korea government (MSIT) (No. NRF-2021R1F1A1056527). This work was partly supported by 2022 University of Seoul Research Grant. This work was partly supported by a clinical research fund of Seoul National University Boramae Hospital.

References

1. Awano T, Sakatani K, Yokose N, Kondo Y, Igarashi T, Hoshino T, et al. : Intraoperative EC-IC bypass blood flow assessment with indocyanine green angiography in moyamoya and non-moyamoya ischemic stroke. **World Neurosurg 73 :** 668-674, 2010
2. Bagher-Ebadian H, Nejad-Davarani SP, Paudyal R, Nagaraga TN, Brown S, Knight R, et al. : Construction of a model-based high resolution arterial input function (AIF) using a standard radiological AIF and the Levenberg-Marquardt algorithm. **Proc Intl Soc Mag Reson Med 19 :** 3902, 2011
3. Calamante F, Thomas DL, Pell GS, Wiersma J, Turner R : Measuring cerebral blood flow using magnetic resonance imaging techniques. **J Cereb Blood Flow Metab 19 :** 701-735, 1999
4. Chen SF, Kato Y, Oda J, Kumar A, Watabe T, Imizu S, et al. : The application of intraoperative near-infrared indocyanine green videoangiography and analysis of fluorescence intensity in cerebrovascular surgery. **Surg Neurol Int 2 :** 42, 2011
5. Dashti R, Laakso A, Niemelä M, Porras M, Hernesniemi J : Microscope-integrated near-infrared indocyanine green videoangiography during surgery of intracranial aneurysms: the helsinki experience. **Surg Neurol 71 :** 543-550; discussion 550, 2009
6. de Oliveira JG, Beck J, Seifert V, Teixeira MJ, Raabe A : Assessment of flow in perforating arteries during intracranial aneurysm surgery using intraoperative near-infrared indocyanine green videoangiography. **Neurosurgery 62(6 Suppl 3) :** 1300-1310, 2008
7. Ferroli P, Acerbi F, Tringali G, Albanese E, Broggi M, Franzini A, et al. : Venous sacrifice in neurosurgery: new insights from venous indocyanine green videoangiography. **J Neurosurg 115 :** 18-23, 2011
8. Foley JP, Dorsey JG : A review of the exponentially modified gaussian (EMG) function: evaluation and subsequent calculation of universal data. **J Chromatogr Sci 22 :** 40-46, 1984
9. Foster SG, Embree PM, O'Brien WR : Flow velocity profile via time-domain correlation: error analysis and computer simulation. **IEEE Trans Ultrason Ferroelectr Freq Control 37 :** 164-175, 1990
10. Gelisken F, Inhoffen W, Schneider U, Stroman GA, Kreissig I : Indocyanine green videoangiography of occult choroidal neovascularization: a comparison of scanning laser ophthalmoscope with high-resolution digital fundus camera. **Retina 18 :** 37-43, 1998
11. Golubev A : Exponentially modified gaussian (EMG) relevance to distributions related to cell proliferation and differentiation. **J Theor Biol 262 :** 257-266, 2010
12. Grushka E : Characterization of exponentially modified gaussian peaks in chromatography. **Anal Chem 44 :** 1733-1738, 1972
13. Hänggi D, Etminan N, Steiger HJ : The impact of microscope-integrated intraoperative near-infrared indocyanine green videoangiography on surgery of arteriovenous malformations and dural arteriovenous fistulae. **Neurosurgery 67 :** 1094-1103; discussion 1103-1104, 2010
14. Iida H, Kanno I, Miura S, Murakami M, Takahashi K, Uemura K : Error analysis of a quantitative cerebral blood flow measurement using H2(15) O autoradiography and positron emission tomography, with respect to the dispersion of the input function. **J Cereb Blood Flow Metab 6 :** 536-545, 1986
15. Jerosch-Herold M, Swingen C, Seethamraju RT : Myocardial blood flow quantification with MRI by model-independent deconvolution. **Med Phys 29 :** 886-897, 2002
16. Kalambet Y, Kozmin Y, Mikhailova K, Nagaev I, Tikhonov P : Reconstruction of chromatographic peaks using the exponentially modified gaussian function. **J Chemom 25 :** 352-356, 2011
17. Kety SS, Schmidt CF : The nitrous oxide method for the quantitative determination of cerebral blood flow in man: theory, procedure and normal values. **J Clin Invest 27 :** 476-483, 1948
18. Kim K, Isu T, Chiba Y, Morimoto D, Ohtsubo S, Kusano M, et al. : The usefulness of icg video angiography in the surgical treatment of superior cluneal nerve entrapment neuropathy: technical note. **J Neurosurg Spine 19 :** 624-628, 2013
19. Kobayashi S, Ishikawa T, Tanabe J, Moroi J, Suzuki A : Quantitative cerebral perfusion assessment using microscope-integrated analysis of intraoperative indocyanine green fluorescence angiography versus positron

emission tomography in superficial temporal artery to middle cerebral artery anastomosis. **Surg Neurol Int 5 :** 135, 2014
20. Koeppe RA, Holden JE, Ip WR : Performance comparison of parameter estimation techniques for the quantitation of local cerebral blood flow by dynamic positron computed tomography. **J Cereb Blood Flow Metab 5 :** 224-234, 1985
21. Ku DN : Blood flow in arteries. **Ann Rev Fluid Mech 29 :** 399-434, 1997
22. Lee JJ, Powers WJ, Faulkner CB, Boyle PJ, Derdeyn CP : The kety-schmidt technique for quantitative perfusion and oxygen metabolism measurements in the mr imaging environment. **AJNR Am J Neuroradiol 34 :** E100-E102, 2013
23. Li X, McGuffin VL : Theoretical evaluation of methods for extracting retention factors and kinetic rate constants in liquid chromatography. **J Chromatogr A 1203 :** 67-80, 2008
24. Lin W, Celik A, Derdeyn C, An H, Lee Y, Videen T, et al. : Quantitative measurements of cerebral blood flow in patients with unilateral carotid artery occlusion: a pet and mr study. **J Magn Reson Imaging 14 :** 659-667, 2001
25. Motulsky H, Christopoulos A : **Fitting models to biological data using linear and nonlinear regression : a practical guide to curve fitting.** Oxford : Oxford University Press, 2004
26. Motulsky HJ, Ransnas LA : Fitting curves to data using nonlinear regression: a practical and nonmathematical review. **FASEB J 1 :** 365-374, 1987
27. Oda J, Kato Y, Chen SF, Sodhiya P, Watabe T, Imizu S, et al. : Intraoperative near-infrared indocyanine green-videoangiography (ICG-VA) and graphic analysis of fluorescence intensity in cerebral aneurysm surgery. **J Clin Neurosci 18 :** 1097-1100, 2011
28. Olufsen MS, Nadim A, Lipsitz LA : Dynamics of cerebral blood flow regulation explained using a lumped parameter model. **Am J Physiol Regul Integr Comp Physiol 282 :** R611-R622, 2002
29. Raabe A, Beck J, Gerlach R, Zimmermann M, Seifert V : Near-infrared indocyanine green video angiography: a new method for intraoperative assessment of vascular flow. **Neurosurgery 52 :** 132-139; discussion 139, 2003
30. Sbalzarini IF : Modeling and simulation of biological systems from image data. **Bioessays 35 :** 482-490, 2013
31. Schuette AJ, Cawley CM, Barrow DL : Indocyanine green videoangiography in the management of dural arteriovenous fistulae. **Neurosurgery 67 :** 658-662; discussion 662, 2010
32. Shah KJ, Cohen-Gadol AA : The application of flow 800 ICG videoangiography color maps for neurovascular surgery and intraoperative decision making. **World Neurosurg 122 :** e186-e197, 2019
33. Son YJ, Kim JE, Park SB, Lee SH, Chung YS, Yang HJ : Quantitative analysis of intraoperative indocyanine green video angiography in aneurysm surgery. **J Cerebrovasc Endovasc Neurosurg 15 :** 76-84, 2013
34. van der Geest RJ, de Roos A, van der Wall EE, Reiber JH : Quantitative analysis of cardiovascular mr images. **Int J Card Imaging 13 :** 247-258, 1997
35. Wintermark M, Maeder P, Thiran JP, Schnyder P, Meuli R : Quantitative assessment of regional cerebral blood flows by perfusion CT studies at low injection rates: a critical review of the underlying theoretical models. **Eur Radiol 11 :** 1220-1230, 2001
36. Wintermark M, Reichhart M, Thiran JP, Maeder P, Chalaron M, Schnyder P, et al. : Prognostic accuracy of cerebral blood flow measurement by perfusion computed tomography, at the time of emergency room admission, in acute stroke patients. **Ann Neurol 51 :** 417-432, 2002

 https://doi.org/10.3340/jkns.2022.0180